Journal of
NANOSTRUCTURES

An Efficient Pd-Sn Catalyst Supported on MWNTs for Hydrogenation of High Concentrated Acetylene Feedstocks: The Potential Role of Isolated Adsorption Site

E. Esmaeili[a,b,*], A. Rashidi[b]

[a] *Department of Chemical Engineering, Birjand University of Technology, P.O. Box 97175/569, Birjand, Iran.*
[b]*Nano Research Center, Research Institute of Petroleum Industry (RIPI), P.O. Box 18745/4163, Tehran, Iran.*

Abstract

In the present study, tin-promoted Pd/MWNTs nanocatalystwas synthesized via polyol technique for application in hydrogenation of high-concentrated acetylene feedstocks. TEM images showed a restricted distribution of nanoparticles in the range of 3-5 nm. The results indicated that nanoparticles sizes were resistant to further catalyst deactivation. XRD patterns signified alloying between Pd and Sn which contained a high percentage of ordered intermetallic structures (70.8%), as confirmed by XPS. According to the results, pore blocking and/or fouling was known as the main reasons of the catalyst deactivation. Here, we supposed a novel deactivation mechanism based on which dehydrogenation susceptibility of carbonaceous species (green oil) played a significant role in the formation of the isolated adsorption sites and then, catalyst deactivation.

1. Introduction

The presence of small amounts of acetylene in ethylene derived from cracking leads to the poisoning of the polymerization catalyst [1-2]. With the best of our knowledge, hydrogenation is found to be a proper method to remove the residue acetylenic species [1-2]. However, low concentration of acetylene in ethylene-rich feedstocks is the main feature of this kind of hydrogenation reaction, the use of acetylene-rich feedstocks has been documented in different studies [3-4]. Recently, Mamadov et al. [4] proposed a method based on which high concentration acetylene feedstocksare hydrogenated to ethylene. As they reported, either fixed bed reactors or wash coated ones are proper for the selective hydrogenation of acetylene to ethylene. Also, some authors have investigated the effect of high concentrated streams of acetylene on durability of the catalyst; however, the main aim of

their investigation was to produce liquid hydrocarbons. Alkhawaldeh et al. [5] inquired into the deactivation behavior of zeolite-supported catalysts during the conversion of methane, acetylene or ethylene in the presence of hydrogen ($H2/C_2H_2$=2.5). According to their investigations, the catalyst deactivation was the major problem of catalysis; leading to the life time of about 3 h. Trimm et al. [6] studied deactivation behavior of Ni/SiO_2 catalyst in oligomerization of acetylene using hydrogen with a volumetric ratio of H_2/C_2H_2 of 3. They observed a complete conversion of acetylene over a period of 5 h at 140 ^{o}C; however, the augmentation of temperature led to the catalyst deactivation.

The considerable role of the isolated adsorption sites in catalysis has been already investigated [7-10]. According to literature [7-8], there are two ways to form the isolated adsorption sites, i.e. via the synthesis of the structured intermetallic compounds and also, through the management of the carbonaceous species resulted from the acetylene conjugation. It is obvious that the ordered intermetallic compounds are different from alloys which are composed of a mixture of metals, intermetallic compounds and/ or non-metals [8].

Crystal growth/sintering, fouling, leaching and poisoning are of great importance in deactivation of the catalyst [11-12]. According to literature [11, 13], the amount of coke accumulated on the catalyst surface is not an essential factor in deactivation degree, but, the nature and the position of coke on the catalyst have significant influences. Menon [14] has classified the cokes to four different types based on their behavior; i.e. harmful, harmless, invisible and beneficial. There are some reports [15-16] in which coke deposited on the metal active sites enhanced the selectivity to

desired products and subsequently, durability of the catalyst.

Recently, carbon nanotubes have displayed promising results in catalysis as catalyst or catalyst support due to their special structure, large specific surface area, hollow and layered structures, extraordinary mechanical and unique electronic properties [17]. According to Bazzazzadegan et al. [18], the carbon nanostructured (CNS) materials could change the governing mechanism towards hydrogen transfer in acetylene hydrogenation reaction. The electronic behavior of carbon nanotubes as electron donors or acceptors reveals that they are able to promote the electron transfer [19-20]. This may be attributed to the curvature of the graphene sheet, modification of the □-electron cloud and then, development of the charge transfer between metal and carbon. Therefore, the molecular adsorption on the metallic phase is improved [17, 21]. Furthermore, the inertness of the carbon support is a property that leads to the formation of lower coke values in comparison with alumina or silica supports [22]. According to literature [23-27], carbon nanostructured materials used in hydro-treating reactions presented higher catalytic activities and less amounts of green oil compared to those of conventional alumina-supported catalysts. Rodriguez [28] rationalized that it is associated with the inertness characteristic of carbon supports. Nowadays, the use of promoters is very common to improve catalytic reactions. Tin promoter is usually applied in dehydrogenation reactions; however, there are some reports on its application in hydrogenation reactions as well [29-30]. In the current study, the effect of temperature on deactivation behavior of Sn-promoted Pd catalyst in hydrogenation of highly concentrated acetylene streams is investigated.

2. Experimental procedure

Carbon nanotubes were prepared by a chemical vapor deposition (CVD) of methane over Co-Mo/MgO at 900 $^{\circ}$C, as already described elsewhere [31]. Afterwards, the carbon nanotubes were purified by washing in an aqueous solution of HClwith the same concentrations of water and then, in HNO$_3$diluted four times by water to remove the impurities, relatively. Subsequently, in order to obtain high dispersions of the metal active sites, the resulted MWNTs were functionalized under sonication for 3 h in a mixture of sulfuric and nitric acids with a volumetric ratio of 3 and 1, respectively.

In this study, we applied polyol method to synthesize the catalysts, according to what already ascribed by our groups [32]. Firstly, functionalized MWNTs were dispersed in ethylene glycol (EG, Merck) by sonication for 30 min. An aqueous solution of metal precursors (PdCl$_2$, SnCl$_2$.2H$_2$O, Merck) was then added slowly to this solution under vigorous stirring. Following the pH adjustment at 12, the solution was rapidly heated up to 140 $^{\circ}$C under reflux. The situation has been kept constant for 3 h, when argon gas was introduced (30 mL/min) into the reaction mixture. In order to obtain a narrow particle size distribution, rapid cooling was necessary. Finally, the resulted black solid was filtered and washedby abundant deionized water and dried in a vacuum oven at 90 $^{\circ}$C for 4 h. For all the catalysts, the molar ratio of Sn to Pd of 1 and Pd loading of 0.1 wt% was considered, except for XRD and XPS analyses with a Pd loading of 5 wt%.

Catalytic activity experiments were carried out in a stainless steel vertical reactor, having 1/4" outer diameter. 0.1 g catalyst powder diluted bySiC for each experiment was applied. Argon gas (70

%vol.) was utilized to dilute the gas feedstocks of H$_2$ to C$_2$H$_2$ with volumetric ratio of 2 and GHSV of about 33000 h^{-1}. The reaction temperature was held in the temperature range of 145-250 $^{\circ}$C. To guarantee the isothermal condition upon the exothermic reaction, an oil bath with a large thermal mass was used. The outlet gas of the reactor was analyzed by gas chromatography using a Shimadzu chromatograph with an alumina packed column. The conversion of acetylene and selectivity to ethylene and ethane in the hydrogenation reaction were defined as below.

$$\text{Conversion (\%)} = \frac{F_{i,ac} - F_{o,ac}}{F_{i,ac}} \times 100$$

$$\text{Selectivity to ethylene (\%)} = \frac{F_{o,ey}}{F_{i,ac} - F_{o,ac}} \times 100$$

$$\text{Selectivity to ethane (\%)} = \frac{F_{o,ea}}{F_{i,ac} - F_{o,ea}} \times 100$$

In these relations, the molar flow is abbreviated as F (mol/min), the subscripts "i" and "o" assign to the feed into and effluent of the reactor. Also, subscripts "ac", "ey" and "ea" refer to acetylene, ethylene and ethane, respectively.A CM-FEG-Philips instrument equipped by an accelerating voltage of 120 keV (TEM) was used to investigate the dispersion and metal particle size of the fresh and the aged catalysts. X-ray diffraction (XRD) with Cu Kα radiation source (Philips PW-1840) was applied to study the crystalline phases of the catalysts and to obtain the average crystallite size of the nanoparticles (by Scherrer's equation). Pore volume measurements were performed by CHEM BET3000 to inquire into the deactivation process upon the acetylene hydrogenation reaction. X-ray photoelectron spectroscopy (XR3E2, 8025-BesTec) was used to find out the chemical states and the relative ratio of the elements on the catalyst surface. Simulation Distillation analysis (SIM DIS,

Varian Simulated Distillation 5.5) was utilized to analyze the condensed green oil effluent of the reactor and the extracted oligomers resulted from the catalyst upon the acetylene hydrogenation reaction. Carbon disulfide was applied to dilute the oligomers examined.

The aged catalysts were also investigated by temperature programmed oxidation (TPO, Micromeritics TPD-2900 apparatus). To prepare the samples for TPO experiment, the fresh catalysts were firstly aged under reaction conditions for 36 h, followed by the exposure to a gaseous mixture (5 vol% air and 95 vol% helium with a flow rate of 50 cm3/min). The heating procedure was performed from the ambient temperature up to 650 ^{o}C at 5 $\circ$C/min. Finally, less strengthen adsorbed species was removed by passing argon over it.Atomic adsorption spectroscopy ((AAS), PerkinElmer) was used to measure the real loaded values of precious catalyst over the support. The percentage of impurities of the catalyst support was determined by an ICP method.

3. Results and discussion

Figs. 1a and b show the TEM images of as-prepared and purified MWNTs, respectively. According to these figures, the purification process could considerably eliminate the impurities. However, ICP measurement confirmed the presence of the residual impurities of below 5% Co–Mo in the catalysts after purification process.

TEM photographs of the un-promoted and PdSn-promoted MWNTs are illustrated in Fig 2. Figs. 2a and b illustrate the changes between the fresh and aged catalysts. According to Figs. 2a and b, further deposition of PdSn nanoparticles on the catalyst surface presents a narrow nanoparticle size distribution in the range of 3-5 nm.
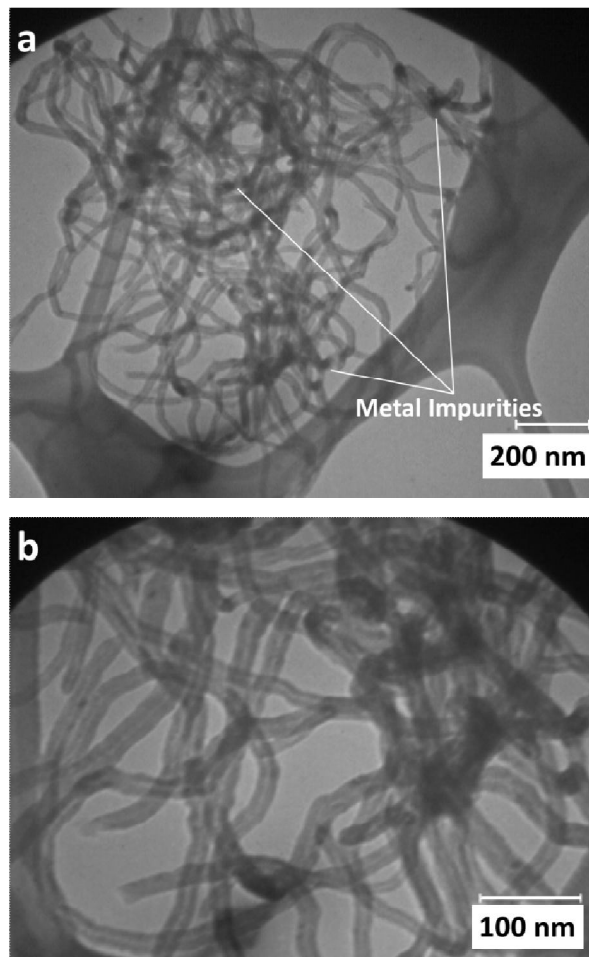

Fig.1. TEM micrographs of a) as-prepared MWNTs and b) purified MWNTs.

According to AAS results, the real contribution of the Pd active site is found to be lower than 1 wt. %; i.e. about 0.78 wt. %. From Fig. 2c, the catalyst aging has no significant influence on nanoparticles sizes; therefore, one may conclude that the crystal growth and/or sintering could not be serious reasons of the catalyst deactivation. This assumption may be supported, when we compare the diameters of the fresh MWNTs (20-40 nm) with the ones aged during the acetylene hydrogenation (45-50 nm). In fact, the increase of diameter of the carbon nanotubes (i.e. ~ 3 nm) may be attributed to the deposition of the coke

precursors on the walls. The entrapped metal active sites disclose that the catalyst deactivation may be originated from pore blocking by oligomers/green oil. Hence, not only the metal active sites inside the pores of MWNTs are affected by deactivation, but the nanoparticles on the external surface of MWNTs are also undergone.

Fig. 3 implies the XRD patterns of MWNTs-supported 5.0 wt. % Pd un-promoted and tin-promoted catalysts. Due to difficulties to characterize the catalysts containing low palladium loading, i.e. 0.1 wt. %, we used 5.0 wt. % Pd, in accordance with literature [33]. The (111) crystallite plane of Pd centroid at 2θ of ca. 40.2° has been indicated as a vertical line in Fig. 3, however, some parts of Pd is in the oxidized state.

According to Fig. 3, the addition of tin results in a slight shift in 2θ values with respect to (111) plane of Pd reflection which confirms the formation of an alloyed phase between Pd and Sn. Because of a very close atomic radius of Pd (1.79 Å) and Sn (1.72 Å), alloying occurs [34].

Pd_2Sn structure is thermodynamically more stabilized in comparison with the other types of the alloys formed between Pd and Sn, i.e. PdSn, $PdSn_2$, Pd_3Sn_2, Pd_3Sn, $PdSn_4$ and $PdSn_3$ [35]. The significant crystallite phase associated with Pd_2Sn is reflected at 39.49° (JCPDS-ICCD, No. 26-1297). The absence of any PdO peaks in the as-prepared tin-promoted XRD pattern may be attributed to the formation of highly surrounded Pd nanoparticles in PdSn alloy lattice.

XPS data of 5.0 wt% Pd catalyst promoted by tin with Sn to Pd molar ratio of 1 is demonstrated in Table 1. According to Table 1, three distinct values related to Sn $3d_{5/2}$ are indicated, which assign to metallic tin (Sn°), Pd-Sn-O and/or Sn-Ophases [36]. The binding energies of 335.1 and 336.4 eV are related to Pd species in metallic andintermetta-
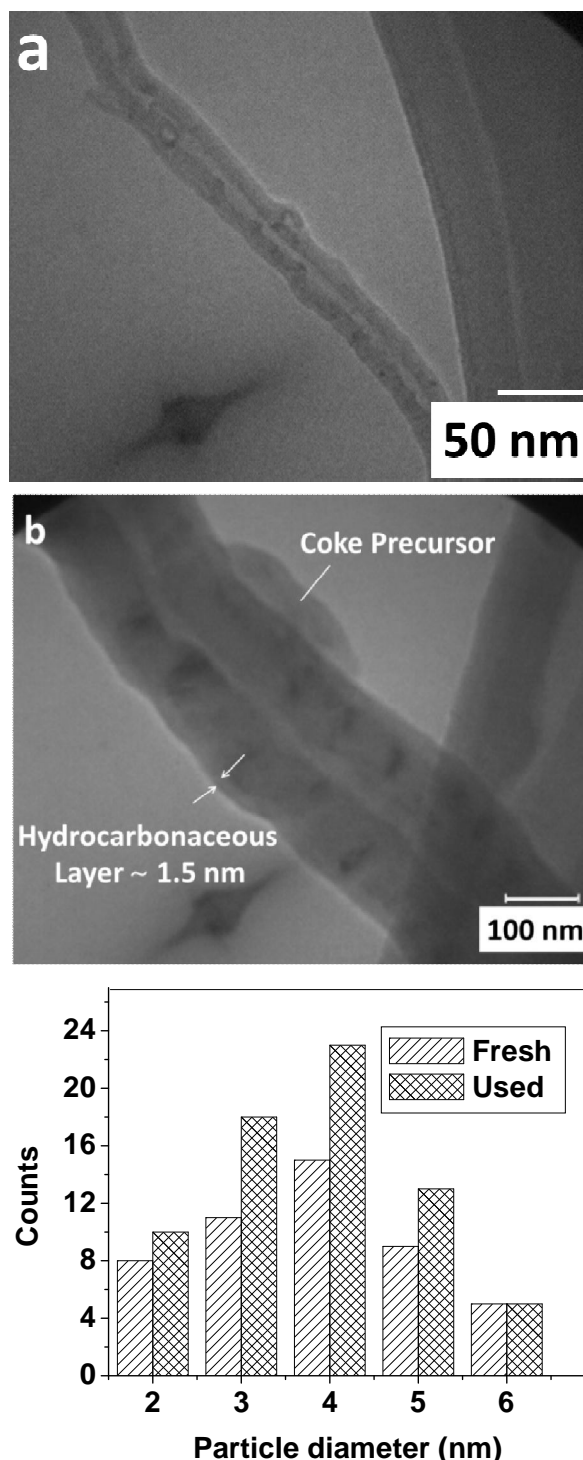

Fig.2. TEM micrographs of a) fresh PdSn/MWNTs, b) aged PdSn/MWNTs, and c) particle diameter histogram of the catalyst before and after aging for 36 h.
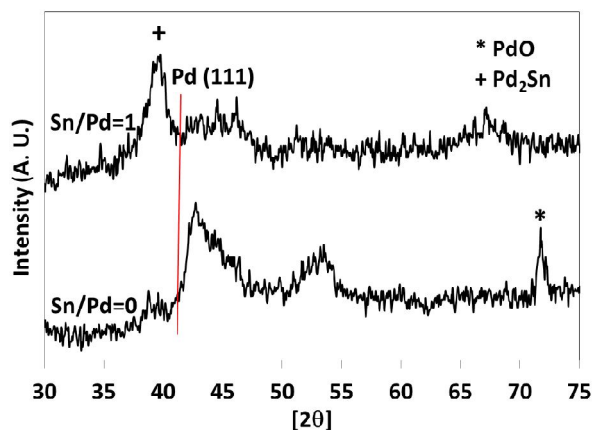
Fig.3. XRD patterns of 5.0 wt% Pd catalysts un-promoted (Sn/Pd=0) and tin-promoted (Sn/Pd=1).

llic states, respectively [7-8]. Since, the presence of Pd_2Sn has been already confirmed by XRD diffraction peaks (see Fig. 3), the stoichiometric contribution of 2:1 may be assumed for the corresponding values of Pd:Sn. To calculate this ratio based on the results of XPS, the peak surface area of zero-valent tin is considered. In line with the results of Table 1, one may observe the value of 4.6, corresponded to Pd/Sn^o. Since, the resulting Pd:Sn ratio derived from XPS is more than the stoichiometric value of 2, the Pd segregation and then, the formation of Pd assembles on the catalyst surface is confirmed [37]. Furthermore, as found from Table 1, the percentage of Pd in intermetallic phase (70.8%) is more pronounced in contrast to the one in metallic form (29.2%).

Table 1. The binding energies of Pd $3d_{5/2}$, Sn $3d_{5/2}$ and the relative percentage of surface species for the 5.0 wt% Pd catalyst promoted by Sn (Sn/Pd=1).

Pd$_{3d5/2}$ eV (%)	Sn$_{3d5/2}$ eV (%)	Pd/Sn^0
Metallic Pd:		
335 (29.2)	Sn^0:485.2 (8.4)	
Intermetallic Pd:	Sn^{2+}: 486.2 (49.4)	4.6
336.4 (70.8)	Sn^{4+}: 487.4 (41.7)	

To find out how much the pore volume of the catalyst is changed upon acetylene hydrogenation

reaction, we measured the pore volumes of the catalyst at different times of reaction, as reported in Table 2. According to Table 2, the pore volume of the fresh catalyst is found to be 0.53 cm^3/g; meanwhile, the values of 0.51, 0.49, 0.46 and 0.37 cm^3/g are obtainedduring aging for 8, 19, 26 and 36 h, respectively. As observed in Table 2, the pore volumes are considerably affected in the range of 26-36 h, as the lost pore volumes are corresponded to 13.2% and 30.2% for the aging times of 26 and 36 h, respectively. This is indicative of the filling or blocking the catalyst pores by the oligomers/green oil during the reaction.

Table 2. Pore volume measurements of tin-promoted Pd catalyst at different reaction times (T=180 ^{o}C, Sn/Pd=1).

Reaction time (h)	Pore volume (cm^3/g)	Pore volume occupied (%)
0	0.53	0
8	0.51	3.8
19	0.49	7.5
26	0.46	13.2
36	0.37	30.2

In Fig. 4, the oligomers effluent of the reactor and the extracted ones from the aged catalysts are evaluated by SIM DIS. To clarify whether the structure of the resulted oligomers at different times of acetylene hydrogenation (9 and 28 h) undergoes any changes, SIM DIS spectra of the exit condensed oligomers are compared. The first peak in the spectra is related to the carbon disulfide as the solvent. According to Fig. 3, no noticeable difference is observed for the exit condensed oligomers after aging of 9 and 28 h. The comparison of the spectra of the condensed oligomers effluent of the reactor and the ones extracted from the catalyst surface reveals the formation of heavier oligomers over the catalyst surface. Because of the permanent production of the oligomers upon the reaction, even at the first

times, and also, the same chemical compositions, one may conclude that the loss of the active sites resulted from pore blocking is known to be as the main reason of catalyst deactivation.
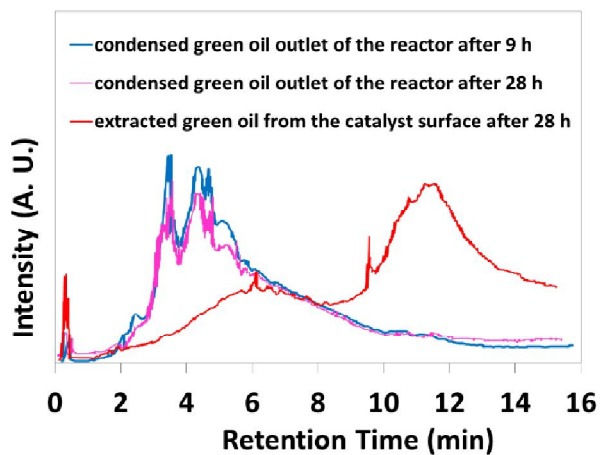

Fig.4. SIM DIS spectra of the condensed outlet green oil of the reactor at 9 and 28 h after the reaction and the oligomers extracted from the catalyst surface upon the acetylene hydrogenation reaction at 150 ^{o}C.

Fig. 5 exhibits the results of TPO spectra of the aged catalyst for 36 h. To identify the peaks of the released species, we neglected the intensity associated with the carbon dioxide resulted from the burning of carbon nanotubes upon the experiment.

According to Fig. 5, there is a peak centered at ca. 210-240 ^{o}C, for the catalyst aged at the reaction temperatures of 180, 210 and 250 ^{o}C. According to literature [15], this peak is attributed to the coke deposited on the metal active site, because the active metal could facilitate coke decomposition. Also, the distinct peak at around 450-470 ^{o}C confirms the presence of coke spelt over from the active site to the support [15]. According to this figure, the surface area of the former peak (i.e. the peak appeared at about 210-240 ^{o}C) is more intensified, when the reaction temperature increases up to 250 ^{o}C. Meanwhile, the intensity of the second peak is decreased with the augmentation of temperature, as it almost disappears for the catalyst aged at reaction temperature of 250 ^{o}C .
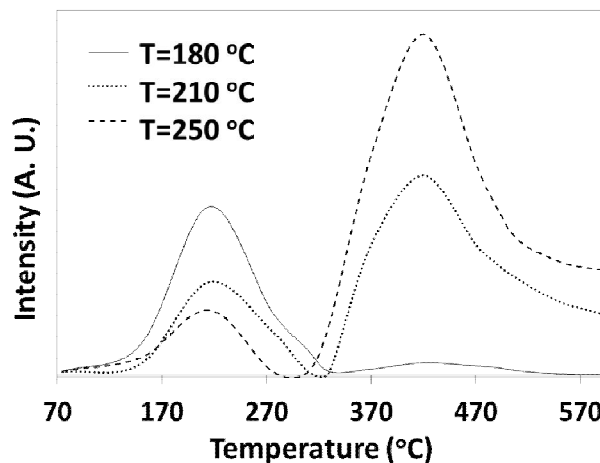

Fig.5. TPO spectra of the catalysts reacted for 36 h at different reaction temperatures.

To evaluate the nature of the green oil/oligomers formed over the catalysts surfaces during the reaction, the extracted green oil from the catalysts surfaces was characterized by FTIR, as shown in Fig. 6. The peaks appeared at ca. 2854 and 2926 cm^{-1} and at about 2873 and 2955 cm^{-1} are respectively associated with the vibration modes of CH_2 and CH_3 groups in the oligomeric chains [38-39]. According to FTIR spectra, higher intensities related to the presence of linear hydrocarbon species (i.e. -CH_2 and -CH_3) are found for the extracted coke from the catalysts reacted at lower temperatures. This may support the formation of less hydrogen-containing oligomers in the coke resulted from the aged catalyst at 250 ^{o}C compared to the results at lower temperatures. This could guide us towards the hydrogen transfer as the governing mechanism in the acetylene hydrogenation reaction. Therefore, a smaller rate of hydrogen transfer via the hydrocarbon layer is expected for the aged catalyst at 250 ^{o}C.

To rationalize our previous suggested hypothesis, we need to refer to the Arrhenius plots. The Arrhenius plot of the catalyst is implied in Fig. 7 which shows a distinct discontinuity for the low and high temperature regions. The activation energies for low (up to 100 ^{o}C) and high temperature region (>100 ^{o}C) are found to be 31.6 kJ/mol and 9.9 kJ/mol, respectively. Some authors observed the same jump in Arrhenius plots for hydrogenation of acetylene [10, 40-41]. McLeod and co-workers [40] obtained the values of 15.9 and 61.9 kJmol^{-1} for the apparent activation energy of acetylene hydrogenation reactions in the high- and low-activity regimes, respectively. According to them [10, 40-41], this may be attributed to two different modes of packing of acetylene molecules over the catalyst surface. In fact, the possibility of the formation of two distinct types of adsorption sites on the catalyst surface is expected. The former is assigned to the isolated adsorption sites, whereas, the latter is connected to the other vacant sites. Therefore, in line with the results illustrated in Fig. 7, a drastic decrease of apparent activation energy may be attributed to the severe changes of acetylene coverages, followed by changing the kinetic regimes. Higher coverages of acetylene may be responsible for the creation of more numbers of the isolated adsorption sites [10, 41].
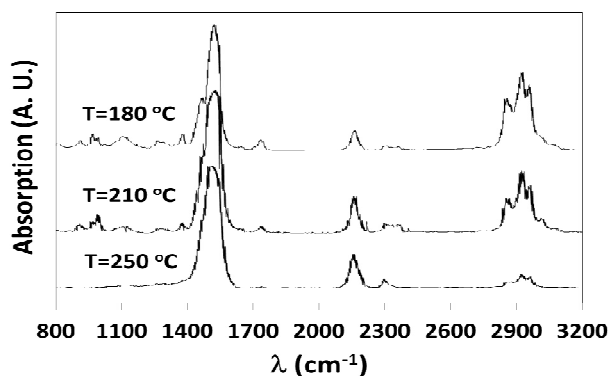
Fig. 8 exhibits the deactivation results of PdSn catalyst at different reaction temperatures vs. time on stream. According to the figure, higher reaction temperatures result in more stabilized catalysts. As shown in Fig. 8, the life times of the catalysts are found to be 4, 23, 39 and 106 h, when the reaction temperatures are varied to 145, 180, 210 and 250 ^{o}C, respectively. Based on the results of Fig. 8, the aged catalyst at 250 ^{o}C, is thoroughly stabilized, even after 106 h. The amounts of selectivities to ethylene are changed vs. time on stream, when the reaction temperature is varied, for instance, the highest value of ethylene selectivity belongs to the catalyst reacted at T=250 ^{o}C; i.e. 98.5±0.5%, whereas, the catalysts examined at lower temperatures (< 250 ^{o}C) result in the values of ethylene selectivities in the range of 93-98%.
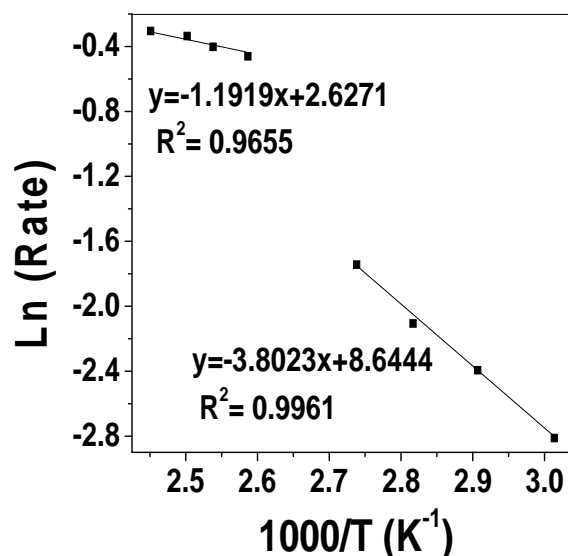

Fig.7. Arrhenius plot of the PdSn/MWNTs at two temperature levels.

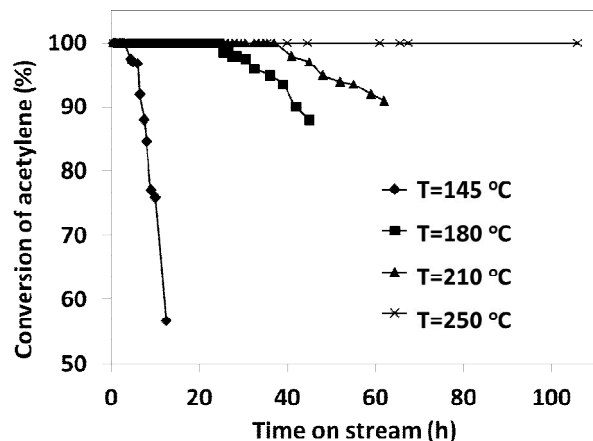**Fig.6.** FTIR spectra of the green oil extracted from the aged catalyst at different temperatures.

Fig.8. Catalytic activities of PdSn catalyst at different reaction temperatures vs. time on stream.

Fig. 9 presents the effect of reaction temperature on the amounts of the condensed green oil in the outlet streams of the applied reactor vs. time on stream. According to Fig. 9, the amounts of green oil resulted from the aging catalyst at 145 ^{o}C is more significant compared to the corresponding values at higher temperatures. For instance, the amount of green oil is measured to be 0.53 mL after 36 h for the catalyst reacted at 145 ^{o}C, meanwhile, the amounts of oilgomers of 0.19, 0.11 and 0.01-0.02 mL are found which are respectively corresponding to the catalysts reacted at 180, 210 and 250 ^{o}C. As mentioned previously, TPO spectra (Fig. 5) showed a clear peak at ca. 210-240 ^{o}C which is associated with the active site-related coke. The amount of this type of coke is indicative of the presence of higher values of carbonaceous species on the catalyst surface. This results in fewer spillovers towards the support, as shown in Fig. 9. It is clear that the presence of carbonaceous species strictly connected to the catalyst surface blocks some Pd sites, which in turn, forms the isolated adsorption sites. As mentioned before [10, 41], the isolated adsorption sites are responsible for higher selectivity to ethylene, lower formation of by-products and thus, longer life time of the

catalyst. Hence, following the existence of more numbers of the isolated adsorption sites, the slower deactivation of the catalyst is expected.
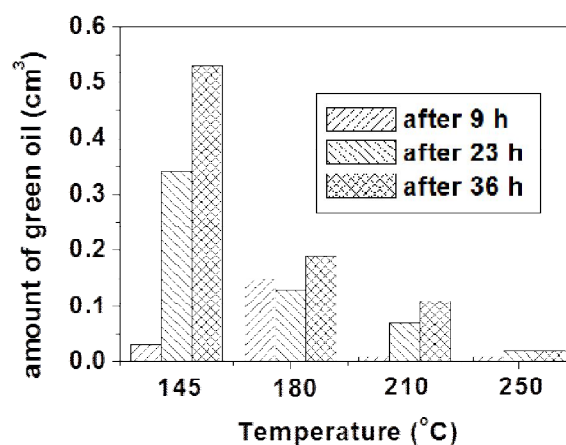

Fig.9. The amounts of condensed green oil outlet from the reactor at different reaction temperatures.

According to McLeod and coworkers [10], the only source of hydrogen in hydrogenation reactions is not limited to the bulk phase, but, dehydrogenation of the adsorbed hydrocarbon species on the metal surface is also efficient. This is in an acceptable accordance with a well-known dehydrogenation characteristic of tin. With the best of our knowledge, tin is usually applied as a promoter in dehydrogenation reactions [42-43]. To find out the origin of the formation of the isolated adsorption sites, we need to start with deactivation mechanism of dehydrogenation catalysts. In general, the coke formation in dehydrogenation reactions includes the adsorption of hydrocarbons on the catalysts surfaces which leads to the formation of coke precursors and thus, further deactivation [44]. However, in the hydrogenation reactions, hydrocarbonaceous species may be useful in selective hydrogenation reaction, but, deactivation of the catalyst in these reactions is attributed to the spillovers of carbonaceous species from the metal active sites to the support. According to some reports [44-47], dehydrogenation reaction shows a decrease in

catalytic activity and also, the life time of the catalyst with an augmentation of the reaction temperature. Therefore, one may expect less capability of PdSn in dehydrogenation of carbonaceous species at high temperatures in selective hydrogenation of acetylene which copes well with what observed in FTIR spectra; i.e. lower intensity of the peaks related to $-CH_2$ and $-CH_3$ for the catalysts aged at higher temperatures.

In the present study, we suggest a novel deactivation mechanism based on which dehydrogenation capability of the metal active site plays a considerable role in selective hydrogenation. This mechanism is illustrated in Fig. 10, emphasizing the concept of the isolated adsorption sites and dehydrogenation ability of the used catalyst. As resulted from what mentioned above, one may find that the governing mechanism of deactivation is based on the formation of the isolated adsorption sites. As we know, the formation of the isolated adsorption sites is attributed to the presence of the ordered intermetallic phases during the catalyst preparation and/or the blockage of Pd-multiple bonded sites using the carbonaceous species upon the reaction. According to literature [7-10], the presence of the isolated adsorption sites resulted from the structured intermetallic compounds has a positive role in the enhancement of the catalyst stabilization in hydrogenation reaction. Therefore, we don't expect any formed green oil/oligomers on the metal active sites by the isolated adsorption sites originated from either the intermetallic structures orthe carbonaceous species. Meanwhile, Pd multiple-bonded sites may be deactivated, when the catalyst is exposed to hydrogenation reactants. According to the schematic presented in Fig. 10, for the isolated adsorption sites, there is just one selective way to hydrogenate acetylene, but, the

hydrogenation of acetylene over the Pd multiple-bonded sites is more complicated. In fact, the formation of a free radical of acetylenicoverlayer could result in long hydrocarbonaceous species connected to two active sites. High dehydrogenation capability of the metal active site may be responsible to spillover the carbonaceous species from the active metal to the support, followed by leaving two active sites which are ready for subsequent formation of carbonaceous species. Therefore, less ability of the active sites to dehydrogenate carbonaceous species may enhance the number of the isolated adsorption sites which in turn, improves the resistance of the catalyst against deactivation phenomena during the reaction. The green oil spelt over from the catalyst surface to the support is able to cover the active sites required for the reaction. The speltoligomers result in decrease of pore volumes due to pore blocking. Therefore, subsequently formed oligomers are placed over the external surface of the support until thoroughly covering of the metal active sites is occurred. Thus, according to these explanations, it may be inferred that the supposed deactivation mechanism is systematically generalized based on the isolated adsorption sites. Further researches are required to suggest a more clarified deactivation mechanism.
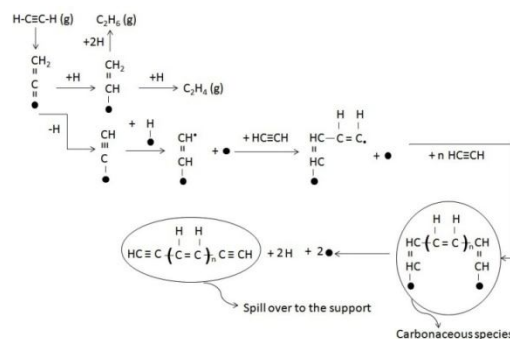

Fig.10. A schematic representation of suggested mechanism of catalyst deactivation during acetylene hydrogenation reaction.

4. Conclusion

Pd-Sn nanoparticles supported on MWNTs were prepared via polyol process technique. TEM micrographs indicated well-dispersed nanoparticles for both the fresh and the aged catalysts which showed the same narrow particle size distribution. Therefore, the main reason of deactivation was found to be pore blocking, confirmed by pore volume measurements. The alloyed catalyst revealed a highly-stabilized behavior in hydrogenation of high concentration acetylene, when the temperature was augmented. This could be attributed to the active site related-coke which was more pronounced with the increased temperature. In fact, dehydrogenation of the presented oligomers on the multiple active sites led to the formation of the isolated adsorption sites. The presence of discontinuity in low and high temperature regions confirmed the existence of two modes of acetylene coverages, including the ordered intermetallic structures and Pd multiple-bonded sites. Conclusively, the isolated adsorption sites resulted from the formation of intermetallic structures along with the ones surrounded by carbonaceous species were responsible to enhance ethylene selectivity and durability of the catalyst.

Acknowledgment

References

[1] J. Panpranot, K. Kontapakdee, P. Praserthdam, Appl. Catal. A 314 (2006) 128-133.

[2] B. Ngamsom, N. Bogdanchikova, M.A. Borja, P. Praserthdam, Catal. Commun. 5 (2004) 243-248.

[3] K.R. Hall, J.A. Bullin, P.T. Eubank, A. Akgerman, R.G. Anthony, US Patent 6,323,247.

[4] A. Mamadov, S. Al-Wahabi, A. Al-Alwan, US patent 8,158,837 B2.

[5] A. Alkhawaldeh, X. Wu, R.G. Anthony, Catal. Today 84 (2003) 43-49.

[6] D.L. Trimm, I.O.Y. Liu, N.W. Cant, J. Mol. Catal. A 288 (2008) 63-74.

[7] K. Kovnir, J. Osswald, M. Armbruster, D. Teschner, G. Weinberg, U. Wild, A. Knop-Gericke, T. Ressler, Y. Grin, R. Schlogl, J. Catal 264 (2009) 93-103.

[8] K. Kovnir, M. Armbruster, D. Teschner, T.V. Venkov, F.C. Jentoft, A. Knop-Gericke, Y. Grin, R. Schlogl, Sci. Tech. Adv. Mater. 8 (2007) 420-427.

[9] A. Borodzinski, A. Golebiowski, Langmuir 13 (1997) 883-887.

[10] A.S. McLeod, R. Blackwell, Chem. Eng. Sci. 59 (2004) 4715-4721.

[11] P. Albers, J. Pietsch, S.F. Parker, J. Mol. Catal. A 173 (2001) 275-286.

[12] C.H. Bartholomew, Appl. Catal. A 212 (2001) 17-60.

[13] P.G. Menon, Chem. Rev. 94 (1994) 1021-1046.

[14] P.G. Menon, J. Mol. Catal. 59 (1990) 207-220.

[15] Y. Azizi, C. Petit, V. Pitchon, J. Catal. 256 (2008) 338-344.

[16] A. Fasi, J.T. Kiss, B. Torok, I. Palink, Appl. Catal. A 200 (2000) 189-200.

[17] P. Serp, M. Corrias, P. Kalck, Appl. Catal. A 253 (2003) 337-358.

[18] H. Bazzazzadegan, M. Kazemeini, A.M. Rashidi, Appl. Catal. A 399 (2011) 184-190.

[19] G.U. Sumanasekera, J.L. Allen, S.L. Fang, A.L. Loper, A.M. Rao, P.C. Eklund, J. Phys. Chem. B 103 (1999) 4292-4297.

[20] M. Iurlo, D. Paolucci, M. Marcaccio, F. Paolucci, Chem. Commun. 40 (2008) 4867-4874.

[21] H. Ma, L. Wang, L. Chen, C. Dong, W. Yu, T. Huang, Y. Qian, Catal. Commun. 8 (2007) 452-456.

[22] M.A. Fraga, E. Jordao, M.J. Mendes, M.M.A. Freitas, J.L. Faria, J.L. Figueiredo, J. Catal. 209 (2002) 355-364.

[23] J.C. Duchet, E.M.V. Oers, V.H.J.D. Beer, R. Prins, J. Catal. 80 (1983) 386-402.

[24] P. Arnoldy, E.M.V. Oers, V.H.J.D. Beer, J.A. Moulijn, R. Prins, Appl. Catal. 48 (1989) 241-252.

[25] V.H.J.D. Beer, F.J. Derbyshire, C.K. Groot, R. Prins, A.W. Scaroni, M. Solar, Fuel 63 (1984) 1095-1100.

[26] A.V. Scaroni, R.G. Jenkins, P.L. Walker, Appl. Catal. 14 (1985) 173-183.

[27] W.G. Augustyn, R.I. MCrindle, N.J. Coville, Appl. Catal. A 388 (2010) 1-6.

[28] F. Rodriguez-Reinoso, Carbon 36 (1998) 159-175.

[29] A. Hammoudeh, S. Mahmoud, J. Mol. Catal. A 203 (2003) 231-239.

[30] J.P. Dath, W. Vermeiren, US patent 7,294,604 B2.

[31] R. Arasteh, M. Masoumi, A.M. Rashidi, I. Moradi, V. Samimi, S.T. Mostafavi, Appl. Surf. Sci. 256 (2010) 4447-4455.

[32] E. Esmaeili, Y. Mortazavi, A.A. Khodadadi, A.M. Rashidi, M. Rashidzadeh, Appl. Surf. Sci. 263 (2012) 513-522.

[33] P. Praserthdam, B. Ngamsom, N. Bogdanchikova, S. Phatanasri, M. Pramotthana, Appl. Catal. A 230 (2002) 41-51.

[34] R.M. Modibedi, T. Masombuka, M.K. Mathe, Int. J. Hydrogen Energy 36 (2001) 4664-4672.

[35] A.F. Lee, C.J. Baddeley, M.S. Tikhov, R.M. Lambert, Surf. Sci. 373 (1997) 195-209.

[36] J. Arana, P.R.D.L. Piscina, J. Llorca, J. Sales, N. Homs, Chem. Mater. 10 (1998) 1333-1342.

[37] F. Geobaldo, G. Spoto, S. Bordig, C. Lamberti, A. Zecchina, J. Chem. Soc. Faraday Trans. 93 (1997) 1243-1249.

[38] A. Dogan, G. Siyakus, F. Severcan, Food Chem. 100 (2007) 1106-1114.

[39] R.B. Moyes, D.W. Walker, P.B. Wells, D.A. Whan, Appl. Catal. 55 (1989) L5-L8.

[40] A.S. McLeod, L.F. Gladden, J. Chem. Phys. 110 (1999) 4000-4008.

[41] Y.K. Park, F.H. Ribeiro, G.A. Somorjai, J. Catal. 178 (1998) 66-75.

[42] R.D. Cortright, P.E. Levin, J.A. Dumesic, Ind. Eng. Chem. Res. 37 (1998) 1717-1723.

[43] Z. Nawaz, X. Tang, Y. Wang, F. Wei, Ind. Eng. Chem. Res. 49 (2010)1274-1280.

[44] M.P. Lobera, C. Tellez, J. Herguido, M. Menendez, Appl. Catal. A 349 (2008) 156-164.

[45] P. Praserthdam, N. Grisdanurak, W. Yuangsawatdikul, Chem. Eng. J. 77 (2000) 215-219.

[46] M. Larsson, M. Hulten, E.A. Blekkan, B. B. Andersson, J. Catal. 164 (1996) 44-53.

[47] G. Aguilar-Rios, P. Salas, M.A. Valenzuela, H. Armendariz, J.A. Wang, J. Salmones, Catal. Lett. 60(1999) 21-25.